4
Molecular Gels for Tissue Engineering

Jun Yan, Bin Sheng Wong, and Lifeng Kang

4.1
Introduction

A *gel* consists of gelator(s) and solvent(s) and is defined as a substantially dilute cross-linked system which exhibits no flow in the steady state [1]. Its solid-like appearance is caused by the immobilization of solvent molecules in a three-dimensional network created by either physical or chemical forces. At molecular level, solvent molecules are mobile within the three-dimensional network, but their movements are limited by capillary forces and solvent-gelator interactions.

Gels can be classified into different groups depending on their constitution, origin, and the type of cross-linking that links gelator molecules and creates the three-dimensional network of the gel. The solvent can be virtually any liquid including water (hydrogels), oil (organogels), and air (aerogels), while the gelator can be of either natural or synthetic origin. Based on the type of cross-linking, gels can be classified as chemical or physical gels. In a chemical gel, its three-dimensional network is formed through strong chemical covalent bonds among the gelator molecules. In a physical gel, however, its three-dimensional network is formed by non-covalent interactions. Physical gels can be formed by clays, proteins, polymers, and some low-molecular-weight compounds. One feature of these low-molecular-weight compounds is that they can gelate liquid at a concentration of less than 2% w/v [2].

4.2
Low-Molecular-Weight Gelators and Molecular Gels

Originally identified by serendipity in the late 1990s, a number of compounds including urea, amides, nucleobases, porphyrin derivatives, dendrimers, surfactants, sugars, fatty acids, and amino acids were known to form gels [3]. Most of these compounds are small-molecular-weight organic compounds, and they have little in common except they were generally found to self-assemble into fibrous

Soft Fibrillar Materials: Fabrication and Applications, First Edition. Edited by Xiang Yang Liu and Jing-Liang Li.

aggregates. These aggregates, or self-assembled fibrillar networks on nano-scale, are formed as a result of a combination of non-covalent interactions among these low-molecular-weight compounds. As gelation is generally difficult to fully predict, these compounds, which can form gels in organic or aqueous solvents without photo- or ionicinitiation, provide a model system to study the relationship between the structure of a gelator and the gel properties [3]. The studies on these small molecular weight compounds subsequently gained growing popularity, emphasis being on their gelation mechanisms and applications in the medical and pharmaceutical industries, such as controlled drug delivery and scaffolding for tissue engineering [4, 5].

Gels derived from those low-molecular-weight gelators (LMWGs) are collectively referred to as *molecular gels*. However, the definition of molecular gels is not as straightforward as that of the other types of gels. Molecular gels have been referred to as *gelations* derived from LMWGs [6]. This definition is consistent in general with other definitions referring to molecular gels as gelations formed from certain LMWGs through non-covalent interactions [7, 8]. In the classification of gels in the above-mentioned review [6], physical gels, which are gels that are formed through physical non-covalent interactions, are proposed to consist of supramolecular and macromolecular gels. Macromolecular gels refer to gels derived from high-molecular-weight compounds such as polymers and collagens, and supramolecular gels refer to gels derived from LMWGs [6]. However, unlike the above classification, that equates molecular gels to supramolecular gels [6], another review considered supramolecular gels to be synonymous with physical gels [9]. In this chapter, we equate supramolecular gels to physical gels (Figure 4.1). By this definition, molecular gels constitute a subgroup of physical gels that are specifically formed from LMWGs with a molecular mass of less than 3000 Da [9]. A number of gelators with molecular weight more than 3000 Da are also included in this review for the potential applications in tissue engineering [10].

It is worth noting that at the heart of molecular gels are non-covalent interactions. Although most gelators form fibrillar networks in a self-assembled

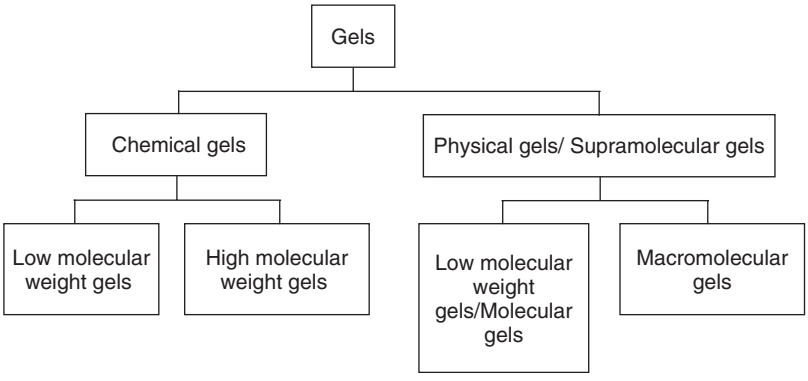

Figure 4.1 Classification of gels.

manner, non-covalent interactions can also be achieved by ionic cross-linking or molecular recognition events such as antibody-antigen and protein-polysaccharide interactions. The reversible bindings between antigen and antibody have been used as a cross-linking mechanism by introducing a type of antigen and its specific antibody into a hydrogel. A gel formed through antigen–antibody binding is stimuli-responsive and swells when it is exposed to a new type of antigen that binds to the same antibody. The non-covalent interactions that form the gel change with the dissociation of the binding between the antibody with its specific antigen and the establishment of binding between the antibodies and the newly introduced antigens [11]. Glycosylated amino acetate types of hydrogelator can form hydrogels with nano-fibers possessing well-developed hydrophobic domains and micro-sized cavities that are filled with immobilized water in a semi-wet hydrogel state. The host–guest binding between the aqueous microcavities and the hydrophobic nanofibers determines the dynamic redistribution of receptor molecules, and these hydrogels can be designed to recognize and discriminate between phosphate derivatives [12].

4.3
Self-Assembly and Gel Structures

Self-assembly is a hierarchical process to form an organized structure from gelator molecules via intermolecular non-covalent interactions, including hydrogen bonds, $\pi-\pi$ stacking, and van der Waals interactions. The final structure occurs in a stepwise manner from intermediate structures formed on the nano-scale through inter-gelator interactions. Gelation is a balance between the tendency of molecules to dissolve or to aggregate in a given solvent. Molecular gels are usually made by heating the gelators in a solvent and cooling down the supersaturated solution to room temperature. As shown in Figure 4.2, the action of cooling causes the

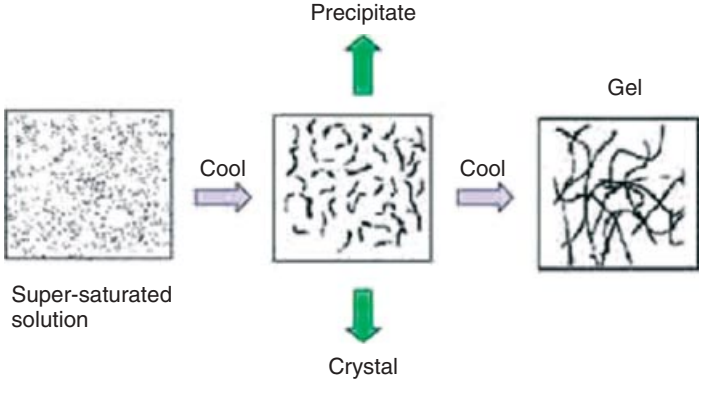

Figure 4.2 Schematic representation of aggregation mode. (Figure adapted from Ref. [6] (Copyright 2004) The Royal Society of Chemistry.)

gelator molecules to condense, leading to one of the three possible situations: crystallization as a result of highly ordered aggregates, amorphous precipitates derived from random aggregation of gelator molecules, or gelation as a result of an aggregation process intermediate between the above-mentioned two processes [6]. Similar to protein structural nomenclatures, primary, secondary, and tertiary structures of a gel, ranging from angstrom to micron, have been proposed to explain the mechanism of gel formation [10].

The *primary structure of a gel* refers to its structure on angstrom to nanometer scale, and is determined by molecular recognitions between complementary donor and acceptor groups in the gelator molecules. During gel formation, LMWGs interact with each other through intermolecular non-covalent interactions, leading to the formation of anisotropic aggregation in one or two dimensions, which serve as platforms for higher-order organization. The driving force for the formation of primary structure of a gel is usually hydrogen bonding in organogels and hydrophobic interactions in hydrogels, as hydrogen bonding loses its strength in aqueous solution [13].

The *secondary structure of a gel* is defined as the morphology, on nano- to micrometer scale, of aggregates such as tapes, ribbons, micelles, and fibers. It is directly influenced by the structure of the gelator molecules. Gelators such as amphiphiles organize in water to generate molecular aggregates in the form of bilayers, spherical or tubular vesicles, and micelles [14]. Some LMWGs form micelles at the critical micellar concentration. As the concentration of gelators increases, these micelles convert into ellipsoidal micelles (disks), and further into cylindrical micellar fibers (rods). These fibers, however, do not necessarily form a gel due to the presence of electrostatic repulsion between charged surfaces.

The tertiary structure of a gel involves the interactions among individual aggregates on micro- to milli-meter scale and determines whether gel or fiber precipitates are formed in a given condition. The formation of a gel, instead of fiber aggregates, is determined by the type of interactions that can occur among the fibers. Compared to shorter fibers, long and flexible fibers are more likely to trap solvent and form a gel. Gels with different properties are made by manipulating the gelation conditions by adding additives or changing the solution temperature to adjust the fibers' morphologies.

In self assembly, LMWGs with complementary donor and acceptor groups can interact with adjacent gelator molecules to form a dimer, which further interact with other dimers to form oligomers. Oligomers extend into fibrils and bundle further into fibers, which in turn entangle into a three-dimensional network, or SAFIN [15]. The self-assembly of an LMWG such as a peptide in a β-sheet conformation is demonstrated in Figure 4.3. In this β-sheet structure, the complementary donor and acceptor groups line up on opposing sides, and interactions between these donor and acceptor groups enable the peptide molecules to assemble themselves in solution into rod-like monomers. These rod-like monomers serve as the foundation of higher hierarchical structures and assemble themselves via recognitions among the complementary donor and acceptor groups into β-sheet tapes and, with increasing concentration, into ribbons (double tapes), fibrils (twisted stacks of

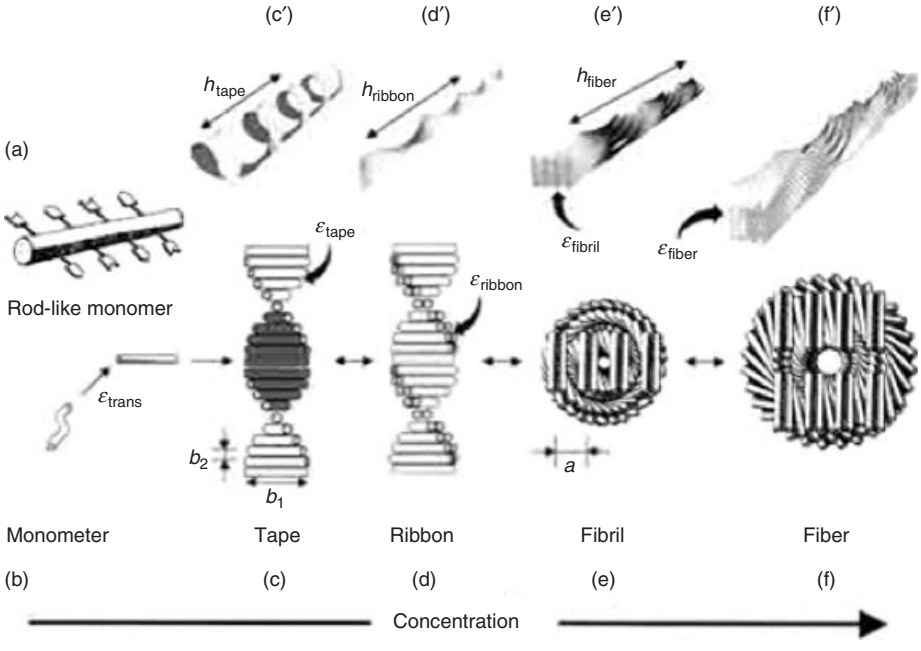

Figure 4.3 Hierarchical self-assembly of gelator molecules. The basic gelator molecules structure (a) as monomer (b) can be assembled into a tape (c and c′) as a result of the interactions among gelator molecules through the complementary donor and acceptor groups within the gelator molecules, shown by arrow. Tapes can form into ribbons (d and d′) by burying hydrophobic residues; ribbons can further assemble into fibrils (e and e′) by lying face to face to form; fibrils assemble side to side to form fibers (f and f′). (Figure adapted from Ref. [16] (Copyright 2001) National Academy of Sciences.)

ribbons), and fibers (entwined fibrils) [16]. In other words, LMWGs are able to form in one dimension an ordered structure through molecular recognitions, and hierarchical structures such as tape, ribbon, fibril, and fibers can be formed on top of these one-dimensional structures LMWGs are able to form ordered structures in one dimension in solution, which underlies their ability to self-assemble into a gel. Ionic self-complementary peptides, for example, form β-sheets in one dimension in solution [17]; Saccharide-based gelators such as glycosylated amino acids, when dissolved in water, form a hydrogen-bonding network in one dimension in the opposite direction, similar to the anti-parallel β-sheet found in proteins [18].

4.4 Applications of Hydrogels in Tissue Engineering

Given their physical properties, which cause them to resemble living tissues, hydrogels have long been used in the medical and pharmaceutical industries

since they were first introduced as soft contact lens material in the 1960s. Hydrogels have been demonstrated for their applications as cell-containing scaffolds for tissue engineering and regeneration by delivering cells into injured areas and reconstructing organs in similar shapes [19–21]. Cells can form only two-dimensional layers in culture; the formation of three-dimensional structures for the purpose of tissue or organ regeneration is made possible by seeding the cells on a three-dimensional scaffold so that they can attach and grow into a designed shape. Additionally, hydrogels can be used as a cell culture system to generate patterned cell arrays for high-throughput screening studies in tissue engineering and drug discovery [22]. However, conventional hydrogel systems also face challenges for tissue engineering applications. For example, one concern is the cyto-toxicity generated during gelators' cross-linking by photo-initiation. Secondly, reagents for ionic cross-linking can induce exchanges of ions with other ionic molecules present in the aqueous environment, compromising the properties of the hydrogel [23].

Unlike covalent cross-linkings, which are hard to break down, physical cross-linkings can be formed via hydrophobic interactions, hydrogen bonding, crystallization, and host–guest inclusion complexation, which can be broken down easily. Despite the lower stability and associated lower mechanical strength, physical cross-linking offers highly versatile and stimuli-responsive hydrogels compared to conventional chemical hydrogels. Self-assembly eliminates the challenges of stable cross-linkings and makes molecular gel an attractive approach to design and construct a three-dimensional network. In this way, gelators capable of self-assembly could contribute to a desired purpose by offering a scaffold in three dimensions with adjustable shape, size, and surface chemistry [24]. Reversibility represents another advantage of molecular gels. Molecular gels can easily be degraded into their building blocks upon a variety of treatments, making them responsive to changes in the environment and amenable to manipulations for specific applications.

One of the major advantages of LMWGs is the ability to flexibly manipulate the fiber network structures responsible for gel formation to achieve different macroscopic properties. For instance, *N*-lauroyl-L-glutamic acid di-*n*-butylamide (GP-1) is an amino-acid derivative capable of gelling many solvents, including propylene glycol, isostearyl alcohol, benzyl benzoate, 1,2-propanediol, and octanol. The gelling mechanisms of GP-1 in these solvents have been extensively studied, and various ways of manipulating the fiber network and fine-tuning the gels' macroscopic properties have been discovered. The degree of fiber branching of GP-1-containing molecular gels can be controlled by many factors such as supersaturation, additives, and ultrasound. Degree of supersaturation plays a critical role in directing the formation of GP-1 fibers. As the temperature of gelation decreases, the degree of supersaturation in the saturated solution increases, leading to enhanced structural mismatch and tip branching, resulting in the formation of highly branched spherulithic networks. This is in stark contrast to the situation at a lower degree of saturation (i.e., higher gelation temperature), where the formation of less highly branched fibrillar networks is encouraged [25].

Non-ionic surfactants such as polyoxyethylene sorbitan monooleate and sorbitan monolaurate increase the degree of fiber branching by selectively adsorb at the growing GP-1 fiber tips and hinder normal fiber growth in one-dimensional axial orientation. Formations of stronger interconnected fiber networks are promoted without affecting the fiber's crystalline nature [26, 27]. Similarly to surfactants, rigid polymer additives such as ethylene/vinyl acetate copolymer and poly(methyl methacrylate comethacrylic acid) also adsorb strongly to GP-1 fibers and promote the formation of highly branched multidomain spherulitic networks. Adsorption of polymer molecules also suppresses primary nucleation and inhibits the formation of less highly branched fibers at an early stage of cooling where the temperature is higher and the degree of supersaturation is relatively lower, forming uniform and homogenous highly branched spherulite only networks [28]. Lower nucleation rate also leads to the development of a smaller number of larger spherulites, reducing boundary area and improving network integration, leading to higher viscoelasticity [29]. Ultrasound is another technique to induce stronger gel formation. Ultrasound promotes gelation below critical gelation concentration and favors the formation of homogenous interconnected fiber networks [27]. As the macroscopic properties of molecular gels are highly dependent on their microscopic network structures, the ability to flexibly adjust the gels' structural network makes LMWG an excellent candidate for soft materials development where different physical properties can be attained to suit specific applications.

While most molecular gels have been made in organic solvents, molecular organogel by default is not compatible with the aqueous *in vivo* environment. This review therefore focuses mainly on applications of molecular hydrogel in tissue engineering, and readers are referred to a recent review on the applications of molecular organogel [30].

Interestingly, biomaterials such as amino acids, lipids, and nucleic acids can arrange themselves spontaneously to form highly organized structures when they are used as building blocks. Based on the studies on self-assembly of these biomaterials, a number of variations have been designed and introduced into these biomaterials to make them self-assemble in a controllable manner. Starting with 3-β-cholesteryl-4-(2-anthryl)butanoate (CAB), the discoveries of most LMWGs were serendipitous, and new gelators were developed by modifying the structure of existing parent gelators [31]. There are a number of ways to classify LMWGs, depending on the type and placement of the polar groups [10] or on the essential groups contributing to the non-covalent interactions that maintain the molecular gel [32]. Based on the nature of the interactions responsible for self-assembly, gelators for molecular gels have been classified as conventional amphiphiles, bolaamphiphiles, Gemini surfactants, sugar-based systems, and others [10]. Based on the functional groups that supply the major non-covalent interactions among gelator molecules, the building blocks for molecular gels have been classified into seven groups [32]. Based on the class of bio-functional molecules incorporated for self-assembly, molecular gels have been classified into four groups, namely, peptide/amino acid-based, saccharide-based, lipid-based, and nucleobase-based

molecular gels. This review discusses the strategies to design gelators and explore the present and potential applications of molecular gels in tissue engineering. A list of the gelators discussed in this review can be found in the Appendix at the end of this review.

4.4.1 Peptide-Based Molecular Gels

Peptide-based hydrogels have been widely studied for tissue engineering to promote the delivery and the survival of cells for tissue regeneration in injured areas. Arginine-glycine-aspartic acid (RGD), for instance, is a motif that contributes to cell adhsesion to extracellular matrix (ECM) and was originally included in conventional chemical gels to promote cell adhesion and differentiation. There are generally two types of peptide-based molecular gels: self complementary alternating amphiphilic peptides [33] and peptides amphiphiles. The ionic self-complementary alternating amphiphilic peptides system designed by Zhang and co-workers takes advantage of the self-assembly of these peptides in solution into structures such as β-sheets, α-helices, and coiled coils [17, 33, 34]. Since synthetic hydrogels are extremely hydrophilic and resist the absorption of proteins and the proper exposure of the specific peptide domains for seeded cells to bind to [35], the hydrophobic interactions maintaining the peptide-based molecular gels designed above are able to promote proper incorporation and exposure of specific peptide domains on the gels. Stuppy and co-workers have taken another approach by covalently linking amino acids to other molecules such as an alkyl chain or an aromatic group, and have designed a family of peptides named peptide amphiphiles to make certain functional peptide-based hydrogels [36–38].

Peptides of alternating hydrophilic and hydrophobic amino acid residues tend to form a β-sheet structure. For that reason, alternating amphiphilic-peptide polymers and oligopeptides can adopt β-sheet structures or aggregates. Hierarchical structures such as tapes, ribbons, fibrils, and fibers can be formed on top of the β-sheet structures under physiological conditions. EAK 16 (AEAEAKAKAEAEAKAK), for example, a peptide with alternating hydrophilic and hydrophobic residues in a region of a yeast protein, was found to form an unusual stable macroscopic membrane spontaneously [39]. In the case of arginine–alanine–aspartate (RAD), which mimics the motif RGD, this has alternating repeat units of positively charged residues (arginine) and negatively charged residues (aspartate) separated by hydrophobic residues (alanine) [33]. These peptides have two surfaces when they form into a β-sheet: the polar surface is composed of ionic side chains and the non-polar surface is made up of alanine residues. These ionic side chains are complementary to one another to form a one-dimensional nanostructure. The amino acids bearing opposite charges give rise to ionic pairs, which serve as non-covalent interactions to maintain the β-sheet structure. The formation and stability of the final assembly is facilitated by intermolecular hydrogen bonding, intermolecular ionic bonds,

hydrophobic interactions, overlapping interactions between individual peptides, and coordination of intermolecular ionic bonds by salt ions [33].

Unlike self-complementary alternating amphiphilic peptides, peptide amphiphiles, or peptide-based molecules that can self-organize into nano-fibers, were designed in such a way to ensure that they first assembles into one-dimensional nanostructures under physiological conditions and then into three-dimensional networks possessing a strong hydrophobic nature. A typical peptide amphiphile is composed of four domains: a hydrophobic tail, a β-sheet-forming segment, charged group(s), and bioactive epitope(s). The first three domains ensure the amphiphilic nature of the gel and the molecular packing within a cylindrical geometry formed by the gelator molecules, which allows for high density of biological signals to present on the fiber surface. The last domain is variable and is used to display different peptides of interest on the surface of the three-dimensional network and to carry out designed functions such as enhancing cell adhesion [24]. The applications of these two types of peptide-based gels in tissue engineering are discussed below.

4.4.1.1 Self-Complementary Alternating Amphiphilic Peptides

Self-assembling peptide nano-fiber scaffolds (SAPNS) designed by the Zhang group used alternating positively and negatively charged L-amino acids to generate a scaffold when they are exposed to physiological solutions such as saline, culture media, and cerebrospinal fluid [34]. With the hamster optic tract bridge model as a model for injuries, treatments with SAPNS was shown to reconnect brain tissue after acute injury [34]. Newly grown axons were found to reconnect to the damaged tissues and facilitate the functional return of vision. With over 99% water content, SAPNS is highly hydrated and can fill an irregular injured area before it forms a molecular nano-fiber scaffold. For this reason, SAPNS was proposed as a candidate for tissue regeneration in irregular injured areas such as those found in damaged optic nerves.

The scaffolds made by biopolymer materials like polylactic acid are composed of very fine nanofibers in the range of 10–100 μm [40]. Self-assembling peptides such as RAD16-I were interweaved to make a scaffold, and its ability to promote rat liver progenitor cell differentiation and function were evaluated [41]. Compared to scaffolds made of fibers whose diameters are in the micrometer range, the scaffolds made of RAD16-I peptide, possessing fibers 10–20 nm in diameter, are thinner by 3 orders of magnitude than conventional microfibers, enabling the diameter of the fibers to be close to that of the cells for improved cell encapsulation. The scaffold was also demonstrated to promote the proliferation of normal progenitor cells and enhance cell differentiation. Cells in adherent cultures divide exponentially but lack the expression of surface markers for mature hepatocytes; in contrast, liver progenitor cells in amphiphilic peptide-based scaffold cultures show non-exponential cell growth but display a characteristic hepatocyte morphology and generate cells with mature hepatocyte markers [41].

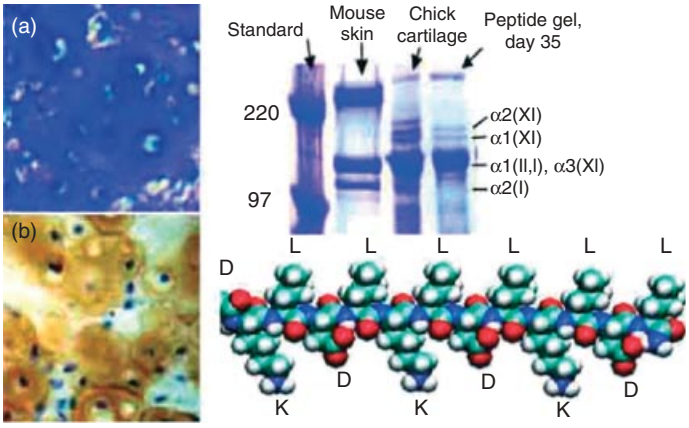

Figure 4.4 Histological and biochemical assessment of the collagen generation in peptide hydrogel encapsulated with chondrocyte. (A) Glycosaminoglycans were detected by toluidine blue staining. (B) Immunohistochemical staining showed the production of type II collagen. (C) Biochemical detection of collagens extracted from samples cultured in peptide hydrogel for 35 days. Standards are the extract from Chick cartilage to show the banding pattern of collagen II and XI. Extract from Mouse skin showed the presence of collagen I α-helix 2 which present in dedifferentiated in fibroblastes but not chondrocytes. (D) Molecular model of KLD-12 peptide shows how the β-sheet structure is formed on the special arrangement of the amino acid residues of the peptide. The backbone of the peptide showed that hydrophilic residues such as lysines-K and aspartic acids (D) are on the bottom of the model; while the hydrophobic residues such as leucines-L are on the top. The alternative appearance of hydrophilic and hydrophobic residues in the backbone of the peptide promotes the formation of β-sheet structure, which in turn promotes the self-assembly through intermolecular interactions. (Figure adapted from Ref. [43] (Copyright 2002) National Academy Sciences.)

The ideal scaffold for cartilage repair is expected to promote cell division and the synthesis of ECM until the repairs reach the stage of tissue maintenance. Hydrogels have been used as a model culture system to study the basic biology of chondrocytes, as the culture of chondrocytes in alginate-containing hydrogels is able to maintain the phenotype of chondrocytes after a number of passages. [42]. A peptide hydrogel scaffold has been developed to encapsulate chondrocytes and to study how the functional cartilage ECM was synthesized within the hydrogel [43], as show in Figure 4.4. Histological studies using specific markers showed that chondrocytes maintained their morphology after being seeded on peptide hydrogel for four weeks.

4.4.1.2 **Peptide Amphiphiles**

The structure and composition of peptide amphiphiles are more flexible than those of amphiphilic-peptide. Designed to function as artificial ECM, peptide amphiphiles were in close connection with markers such as RGD in regenerative medicine. RGD is a peptide motif located on the chain of proteins present in the ECM and has been conjugated to a number of gelators to make synthetic and

natural hydrogels [35]. It binds specifically to integrin, a transmembrane protein that mediates cell adhesion and controls cell adhesion, spread, and migration. The binding between RGD and its receptors can be controlled by manipulating the density of RGD incorporated into the peptide amphiphile by altering the number of RGD peptides added into the amphiphile molecule. High density of RGD was shown to promote receptor clustering and maximize binding between ligands and receptors between scaffold and cells [44].

To direct neuronal cell differentiation, a self-assembling artificial scaffold made from a peptide amphiphile bearing a neurite-promoting laminin marker isoleucine-lysine-valine-alanine-valine (IKVAV) was designed [37]. Next to this peptide marker is a glutamine residue that makes this peptide negatively charged when the pH was adjusted at 7.4, so that the electrostatic repulsion among peptide molecules can be overcome by cations, which facilitates the self-assembly of the peptide when they are exposed to cell suspensions. The β-sheet-forming segment in this peptide is designed as 4 alanine residues and 3 glycine residues and the hydrophobic tail is composed of an alkyl chain of 16 carbons. When four uniformly hydrophobic alanine residues are replaced by an alternating serine-leucine-serine-leucine (SLSL) sequence, the gelation of this new peptide amphiphile takes place at a lower rate than that for the alanine-containing amphiphiles. The self-assembly is driven by intermolecular hydrogen bonding, and the unfavorable contact between hydrophobic segments and water molecules after electrostatic repulsions between peptide molecules are overcome by cations in the cell culture medium [37]. In aqueous, salt-free solution, the secondary structures of the IKVAV-bearing peptide amphiphiles are all dominated by hydrogen-bonded β-sheet structure [38]. The effect of the incorporation of IKVAV epitope was clearly demonstrated by the promotion of neurite outgrowth and the targeted neural differentiation of neuron progenitor cells into neuron but not astrocytes, as demonstrated by staining of cell-type-specific markers.

Heparin-binding peptide amphiphile has been widely used for angiogenesis. Heparin is a highly sulfated glycosaminoglycan and is able to bind many growth factors that promote vessel generation including vascular endothelial growth factor and fibroblast growth factor 2 through the heparin-binding domains. Self-assembled nanostructure forms in a few seconds by mixing a solution of peptide amphiphile designed to bind heparin and a solution of heparin with angiogenic growth factors. Upon changes in the solution pH or the addition of ions with opposite charges to the peptide amphiphile, the peptide amphiphile molecules become charged in aqueous solution and self-assemble into β-sheet cylindrical nanostructures [45]. The addition of heparin to the peptide amphiphile eliminated the charges on the peptide amphiphile molecules and triggered the formation of β-sheet nanostructure, in which the fatty acid tails become hidden in the core and the peptide segments aggregate through hydrogen bonding. As shown in Figure 4.5, this nanostructure was shown to stimulate extensive new blood vessel formation on rat cornea in an *in vivo* angiogenesis assay [46]. The structure has also been shown to facilitate islet transplantation [47] with nanogram amounts of growth-factor proteins, which otherwise cannot induce any detectable angiogenesis.

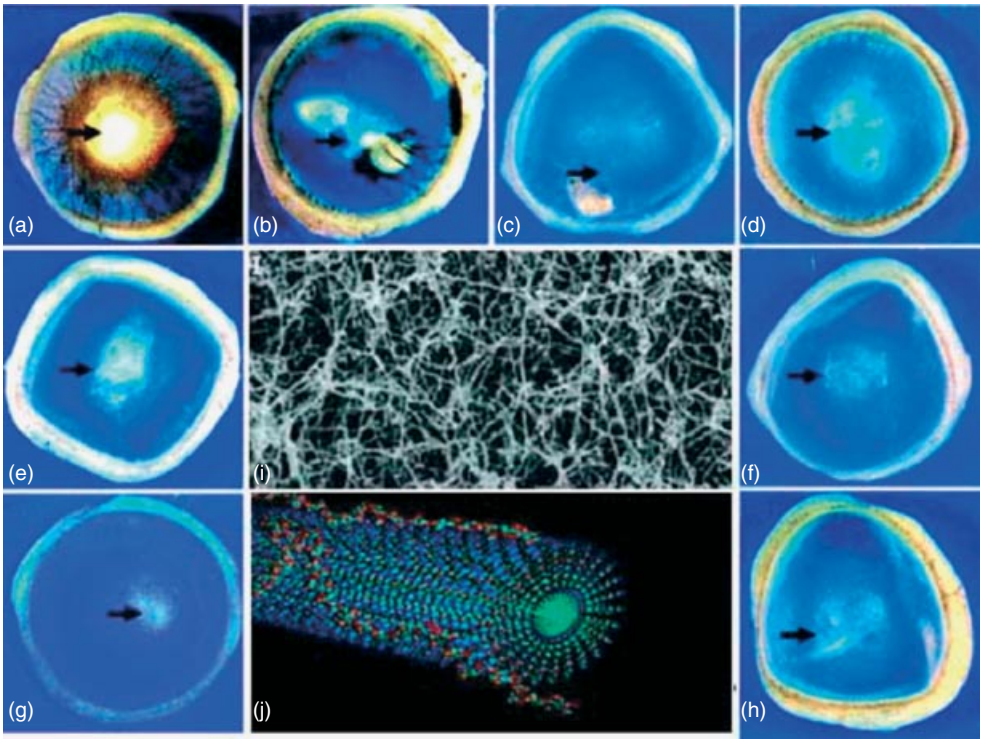

Figure 4.5 Generation of blood vessel on rat cornea. Rat cornea was pictured 10 days for blood vessel generation to assess the effect on angiogenesis by the combination of different materials. (A) Heparin-nucleated PA nanofiber with growth factors; (B) collagen, heparin, and growth factors; (C) collagen with growth factors; (D) heparin with growth factors; (E) collagen with heparin; (F) Heparin-nucleated PA with growth factors; (G) PA-heparin without growth factors; (H) growth factors alone. In sharp contrast to the intensive blood vessel regeneration induced by combinations in A, the combinations in B and C caused some vessel regeneration and the combinations of D to H showed little sign of vessel regeneration. (I) Image under scanning electron microscopy showing the fiber bundles of heparin-nucleated PA nanostructures (scale bar = 2 μm). (J) Diagram shows the cylindrical structure of heparin-nucleated PA. Positively charged PA molecules are able to bind to negatively charged heparin molecules. The aggregation of heparin-nucleated PA finally takes the cylindered structure. (Figure adapted from Ref. [46] (Copyright 2006) American Chemical Society.)

4.4.2 Saccharide-Based Molecular Gels

Saccharide-based molecular assemblies have become attractive in their potential applications in tissue engineering owing to their intrinsic biocompatibility. Saccharides and their glyco-conjugates are rich in ECM, and those on the cell surface play essential roles in traducing signals in and out of a cell.

Compared to peptide-based molecular gels, studies and applications of saccharide-based molecular gels are still limited. Despite their potential as a matrix for cell immobilization and encapsulation, saccharide-based gelators usually have complex structures, which have limited their application for tissue engineering [48].

Investigators' attention to saccharide-based gelators stemmed from the studies on organogels of aliphatic amide derivatives, a typical example of hydrogen bond-based gelators. The analysis of the structures of aliphatic amide derivatives organogels showed that these molecules themselves have complementary donors and acceptors to form intermolecular hydrogen-bonding interactions [49–53]. This observation directed investigators' attention to saccharides, because saccharides can also form hydrogen bonding, and new saccharide-integrated gelators can be readily designed by replacing the hydrogen-bond-forming segment of a parental gelator with a saccharide. Taking a library screening strategy, the Shinkai group examined saccharide-based aggregates by introducing a variety of hydrogen-bond-forming segments into existing gelators by appropriate selection from a saccharide library [49].

Some excellent low-molecular-weight hydrogelators which gelate at a concentration of less than 0.1 wt% were identified from a saccharide library made by solid-phase (glycol)lipid synthesis [54]. The structural studies on the gels derived from one of the gelators showed how the hierarchal assembly of this gelator is formed on top of the one-dimensional fiber structure [18]. On nanoscale, the amphiphilic structure of this gelator leads to a bimolecular layer that is maintained by both hydrophobic tails and hydrogen-bondings. The bimolecular layer further gives rise to thin fibers with a hydrophobic core and an oriented saccharide interface. The thin fibers are entangled and give rise to thick fibers which immobilize water molecules [18]. Thus a hydrogel is formed as a result of self-assembly of a small-molecular-weight gelator and is further applied to distinguish different phosphate derivatives [12]. The hydrogels derived from other excellent saccharide-based hydrogelators have been applied for trace insulin detection [55], or in cell culture for efficient encapsulation and distribution of live Jurkat cells under physiological conditions [56], as shown in Figure 4.6.

Hydrogen bonding is not the only mechanism for saccharide-based gel formation. Saccharide-based glycolipids were reported to form gels in a self-assembly manner when mixed with a 1 : 1 ratio of alcohol/water or acetone/water [57]. These glycolipids dissolved in boiling water, and fine fibers were generated during the period that the solution was gradually cooled down to room temperature. Nano-fiber association and network formation induce efficient gelation, and the gels formed in alcohol/water or acetone/water are thermo-reversible in nature. Interestingly, instead of hydrogen bonding, the driving force for the gel formation process is thought to be $\pi-\pi$ interactions, because the limited number of hydroxyl groups in the glycolipids made hydrogen bonding unlikely to be a dominant force in directing the gel formation in one dimension [57].

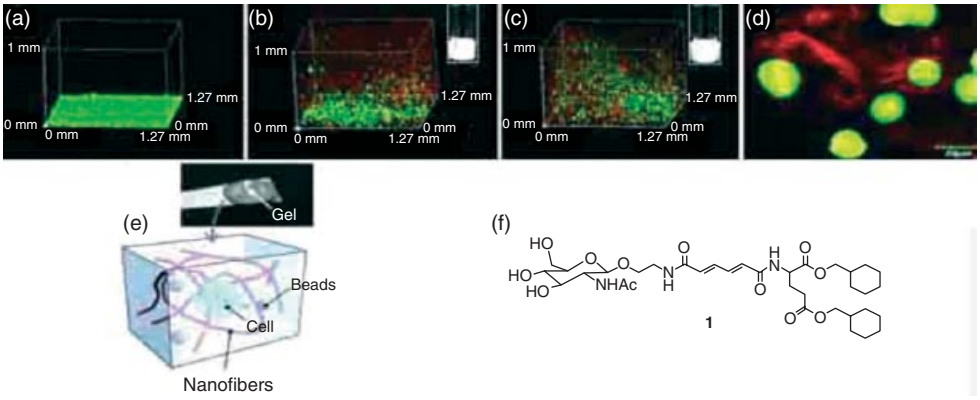

Figure 4.6 3D images of encapsulation of live Jurkat cells in the presence or absence of nanofiber 1 and beads. The Jurkat cell encapsulation was promoted by the presence of nanofiber 1 and further facilitated by the addition of beads which caused even distribution of the nanofiber networks. (A) Jurkat cells in cell culture medium only; (B) Jurkat cells in culture medium and in the presence of nanofiber 1(0.1 wt%); (C) Jurkat cells in culture medium and in the presence of both nanofiber 1(0.1 wt%) and beads. The insets on the top right of the images show images of the cell culture gel 1. The cells and nanofibers were pre-labeled with different dyes. (D) Magnified z-slice image of picture C; (E) The image and the diagram (not drawn to scale) show how the Jurkat cells were prepared to encapsulate in cell culture medium, nanofiber 1(0.1 wt%) in the presence of beads; (F) Chemical formula of the gelator composed of nanfiber 1. (Figure adapted from Ref. [56] (Copyright 2008) John Wiley & Sons, Inc.)

4.4.3 Lipid-Based Molecular Gels

Lipids are present ubiquitously in the biological system, ranging from being a highly efficient source of energy and major constituents of cellular membranes to various hormones and signaling molecules required for cellular growth and differentiation [58]. Due to their prevalence in nature and their inherent biocompatibility and biostability, lipids have been widely studied and researched by the scientific community, particularly in drug delivery and tissue engineering. The ability of lipids, especially those with amphiphilic property, to self-assemble into two- and three-dimensional supramolecular structures further contributed to their potential to be used in material science research [59].

Typically, a lipid comprises three essential features, namely a hydrophobic tail, a polar head, and a backbone that connects the two together [59]. The polar groups found in lipids can be either one or more charge/uncharged polar moieties, while the hydrophobic portions of lipids comprise either aromatic or saturated/unsaturated aliphatic side chains. Lipids are further classified into various subcategories such as phospholipids, isoprenoids, sphingolipids, glycerolipids, and sterol lipids, according to their backbone structures. One interesting property of lipids is their ability to self-associate and self-assemble into specific and ordered

supramolecular structures when placed in a solvent. This phenomenon is in fact not uncommon in nature and can be observed in a variety of chemical and biological systems. Examples of such molecular aggregates and assemblies include monolayers, micelles, liposomes, and bilayers. These structures have successfully found a multitude of clinical applications over the years. Liposomes, for instance, which are self-folded lipid bilayer vesicles with hydrophilic internal core, have been employed successfully for intravenous administration of amphotericin B to combat systemic fungal infections, demonstrating prolonged circulation time and reduced toxicity [60]. Recent attempts at delivering nucleotide sequences with self-assembled liposomes for gene therapy have also shown promising results.

Aside from forming simpler two- and three-dimensional aggregates like micelles and liposomes, several lipids, for example, cholesterols and fatty acids, possess the ability to self-assemble into more complicated tubules and ribbon-like structures, which could interconnect via non-covalent interactions, namely hydrogen bonding, $\pi-\pi$ aromatic stacking, and van der Waals interaction, and form matrix architectures capable of trapping solvents, leading to the formation of physical molecular gels [59].

Diacetylene-containing phospholipid 1,2-bis(10,12-tricosadiynoyl)-*sn*-glycero-3-phosphocholine ($DC_{8,9}PC$) is able to assemble into hollow cylindrical microtubules having a diameter of 0.5 μm and a length of 50–200 μm with one or more bilayers spontaneously [61]. These microcylinders were employed successfully for the encapsulation and release of growth factors for nerve regeneration and osteogenic differentiation [62, 63]. An equimolar mixture of $DC_{8,9}PC$ and 1,2-bis(dinonanoyl)-*sn*-glycero-3-phosphocholine was found to be able to promote the formation of lipid nanotubules with sub-100 nm diameter (a value that is 10 times smaller than the lipid tubules described in previous literature), which transform into helical ribbons upon heating that interconnect in three dimensions and form a physical gel [64]. Detailed analysis of the mechanisms and the properties of the nanotubules formed indicated that the transformation of nanotubule to twisted ribbon is accompanied by an inversion of the circular dichroism signal, which implies that the gelation process involves significant molecular reorganization [65]. With a water content of more than 98%, these lipid-based molecular hydrogels are suitable scaffolding materials for tissue engineering [59]. By combining the abilities of such lipid tubules to release encapsulated growth factors and generate biocompatible hydrogels, it is therefore possible to fabricate growth factor-laden tissue engineering scaffolds that can simultaneously support cell proliferation and guide cellular differentiation.

Although the use of lipid-based molecular gels in tissue engineering remains largely unexplored, a successful attempt of achieving cellular growth and attachment on lipid-based molecular gel has been reported. Lukyanova *et al*. have developed a microporous, biodegradable, and non-toxic organogel cell culture platform with the use of a fatty acid, 12-hydroxystearic acid (HSA), as the organogelator [5]. Two different organic solvents, namely caprylic/capric triglyceride and soybean oil, were gelled with HSA using the particulate leaching method to generate micropores on the scaffolds to facilitate nutrient distribution and enhance cell

penetration [66]. The organogel formed possessed self-assembled fiber-like organization stabilized by non-covalent associations between the fatty acid gelators. A wettability test conducted on the two types of organogels showed similar contact angles of around 74°, which was fairly close to the angle value of 70° needed for cell adhesion [67]. Prior to cell seeding with Chinese Hamster Ovary (CHO) cells, previously sterilized scaffolds were first incubated in culture medium for 24 h to promote nutrient transfer. Cell attachment and proliferation, as measured by 3-(4,5-Dimethylthiazol-2-yl)-2,5-diphenyltetrazolium bromide (MTT) assay on days 1, 3, and 7, were observed to be higher on porous organogel scaffolds than on their non-porous counterparts, suggesting the importance of microporosity in providing high draining, via capillarity effect, to facilitate cell attachment. Histological observations with Masson's trichrome staining revealed the presence of viable CHO cells on top and deep inside the internal porous structures, indicating once again the significance of porosity on cell colonization. Seeded CHO cells were observed to proliferate rapidly after 14 days of incubation before reaching a plateau after 21 days. In addition, the cells were attached to pore walls and were grouped together in a blue-stained fibrous network, which the author has identified as collagen. The round cellular morphology with retracted extension observed further supported the claim that collagen was produced. Figure 4.7 shows the microscopic images depicting successful growth and attachment of CHO cells on the organogel scaffolds. This *in vitro* cell attachment study revealed great potential for lipid-based organogels to not only support cell growth and migration but also to induce collagen and ECM formation.

Conventionally, the ways to control the mechanical and macroscopic properties of molecular gels usually involve adjusting the design, selection, and ratio of gelator and solvent molecules. These modifications have been demonstrated to control mainly the primary and secondary morphological structures of a gel. It is, however, relatively more challenging to alter a gel's tertiary structure to achieve desired macroscopic properties, due to limited understanding of the process involved in the transition of fibrous aggregates to a complex interconnected network [68]. Li *et al*. have looked into the nucleation and fiber growth behaviors of molecular gels, and a method to effectively control the microstructures and macroscopic properties of a molecular organogel (consisting of HSA as the gelator and benzyl benzoate as the organic solvent) by controlling the thermal processing conditions of the gelling process has been successfully devised [69]. It was shown that by increasing supercooling/supersaturation (i.e., decreasing the temperature at which gels are formed), organogels with higher elasticity, shorter correlation fiber length (i.e., branching distance between two neighboring branch points along a fibril), and denser fiber network were obtained at a fixed HSA concentration, as shown in Figure 4.8. With this method, gels with the same elastic modulus and rheological behavior can be fabricated with lower gelator concentration by controlling the degree of supercooling of the system, thereby saving materials. The ability to vary the mechanical and macroscopic properties of molecular gels is important in determining the gels' performance and functions, particularly for

tissue engineering, where the mechanical properties of scaffolds, such as hardness, can have significant impacts on the ability for cells to attach and grow [70].

Although research involving tissue engineering on lipid-based molecular gel scaffolds may seem limited at the present time, there exists significant potential for them to be developed into successful cell culture systems. The use of lipids, either as monomer, liposome, or surface coating, in tissue engineering has provided powerful evidence of their essential roles in guiding cellular development, attachment, and differentiation.

Sphingosine-1-phosphate (S1P), for instance, a key member of the sphingolipids, is pivotal in the induction of numerous cellular processes. S1P is involved in the survival, proliferation, and regulation of apoptosis in human embryonic stem cells [71]. Additionally, S1P maintains growth and multipotency of human bone marrow and adipose tissue-derived mesenchymal stem cells (MSCs) [72]. A recent study involving culturing human umbilical cord MSC with cardiomyocytes-conditioned medium supplemented with S1P showed that S1P is able to trigger and potentiate differentiation and maturation of human umbilical cord MSC into cardiomyocytes.

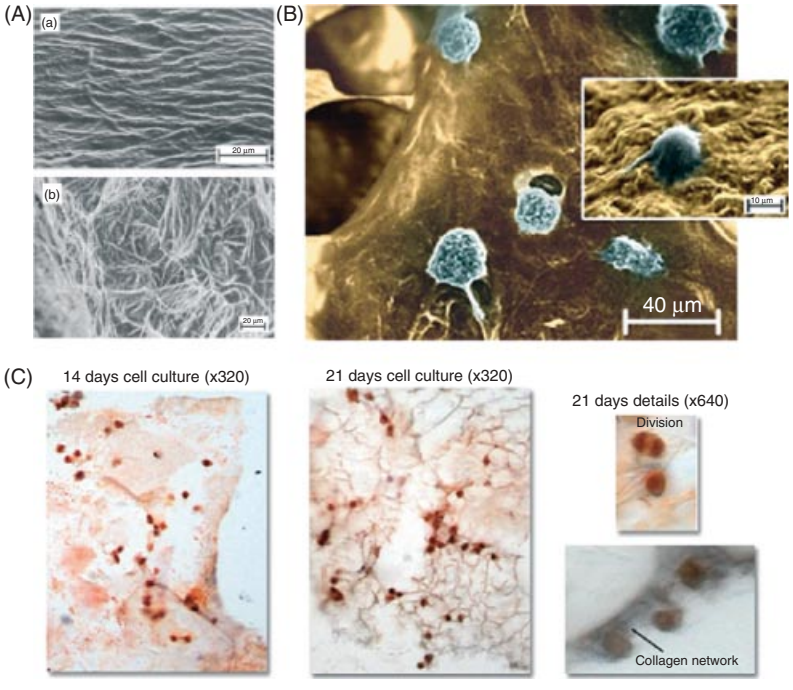

Figure 4.7 (A) SEM micrographs of fibrous nanostructures of soybean oil (a) and caprylic/capric triglyceride organogels (b). (B) Environmental SEM micrographs of CHO cells on a soybean oil based organogel after 21 days of incubation. (C) Histological images showing the morphology and attachment of CHO cells in a soybean oil organogel after 14 and 21 days of cell culture with Masson's trichrome staining; Detailed histological examination revealed ongoing cell division and possible formation of collagen fibrous network. (Figures adapted from Ref. [5] (Copyright 2010) Elsevier B.V.)

Besides possessing cardiomyocyte-like morphology, cells induced by S1P also showed heightened expression of cardiomyocyte markers and the ability to generate atrial type action potential with major voltage gated inward and outward currents [73].

Phosphatidylserine (PS) is another example of a lipid that has found abundant applications in tissue engineering. In addition to its structural role in biological membranes, PS is also heavily involved in the activity of many membrane-bound proteins, such as protein kinase C and Na^+/K^+ ATPase, which are all major players in cell signaling pathways that ultimately determine cell growth and differentiation [74]. An experiment involving incorporation of PS into bioglass-collagen composite scaffolds showed that PS was able to support a higher degree of rat MSC attachment, proliferation, and osteogenic differentiation. *In vivo* implant study further demonstrated excellent biocompatibility and osteoconductivity of the PS-containing scaffolds in rat femur [75].

On hindsight, while the use of lipid-based organogels in tissue engineering is still rather limited, the promising experimental results presented by Lukyanova *et al.*, coupled with the diverse and imperative functions of lipids in cell development and differentiation, have certainly unveiled exciting possibilities for lipid-based molecular gels to be developed into potent tissue engineering scaffolds in the future.

4.4.4
Nucleobase-Based Molecular Gels

Nucleobases have been gaining significant popularity in gels research, owing to their unique abilities to foster directionally controlled multiple intermolecular

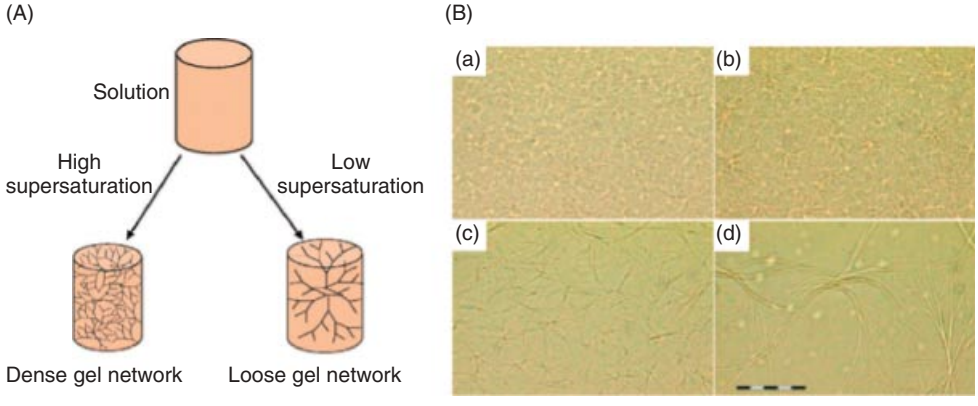

Figure 4.8 (A) Schematic showing thermal engineering of the micro- and nanostructure of a gel by controlling the degree of supercooling during gel formation (B) Microscopic images of the fiber network of 2.5 mol% HAS (12-hydroxystearic acid)-benzyl benzoate gel formed at different temperatures. (a) 20, (b) 40, (c) 50, and (d) 55 °C. Scale bar: 100 μm. (Figures adapted from Ref. [69] (Copyright 2009) American Chemical Society.)

interactions and form geometrically well-designed and organized structures like helixes and lamellar motifs [76]. Non-covalent intermolecular interactions, for instance hydrogen bonds, hydrophobic interaction, and π−π aromatic stacking, serve to bridge individual nucleobases subunits together and form spatially oriented secondary structures, which could further interact and form increasingly intricate tertiary structures, eventually producing extended interconnected networks capable of trapping solvents and forming gels [10]. In this section, two major types of nucleobase-containing gelators, namely nucleobases/nucleobase-containing hybrid biomolecules, and nucleic acid chains, will be discussed. Nucleic acid chains are grouped in a distinct category on their own, as they are structurally more complex than simpler nucleobase monomers and their hybrid structures, and possess some characteristics differing from those of conventional molecular gelators.

4.4.4.1 Nucleobases and Hybrid Biomolecules Containing Nucleobases

Nucleobases are substituted heteroaromatic purines or pyrimidines. Intermolecular non-covalent interactions that can be formed between the nucleobases are pivotal for the self-assembly of molecular structures. The presence of multiple hydrogen bond acceptors and donors within the nucleobases enables them to form relatively strong and directional hydrogen bonding via not only Watson–Crick or Hoogsteen type base pairing, but also other hydrogen bonding patterns like reverse Watson–Crick, reverse Hoogsteen, and Wobble base pairing [77]. π−π stacking perpendicular to the aromatic planes of nucleobases is also important in stabilizing self-assembled structures. In general, the stacking ability between a purine and a purine is the highest, followed by that between a purine and a pyrimidine and lastly between two pyrimidines [78]. There are five main types of nucleobases, namely adenine, guanine, thymine, cytosine, and uracil. Linking the nucleobases to either a ribose or a deoxyribose sugar unit via a β-glycosidic bond yields the nucleosides, adenosine, guanosine, thymidine, cytidine, and uridine, respectively.

Successful gelation attempts have been observed primarily with guanosine derivatives. The formation of G-quartet cyclic tetrameric structures, templated by alkali metal ions, produces homogenous gels. Cyclic tetramers involving guanine moieties are stabilized by hydrogen bonding. These quartets further assemble into columnar stacks, aided by both π−π aromatic stacking and alkali metal ions, and eventually orient themselves in a hexagonal arrangement to form extended molecular networks capable of entrapping solvents [79].

Nucleosides or nucleobases can be incorporated into various other biocompatible and biostable LMWGs, such as peptides, lipids, and steroids, to generate novel hybrid structures with improved gelation ability. Inclusion of nucleosides or nucleobases often enhances intermolecular interactions between the gelating agents by providing additional hydrogen bonding and/or π−π aromatic stacking.

Li *et al.* have successfully synthesized a multifunctional and biocompatible molecular hydrogelator consisting of nucleobases, amino acids, and glycosides [80]. This nucleobases–amino acids–glycosides hybrid is formed by attaching a nucleobase, which can be adenine, thymine, guanine, or cytosine, to the N terminal and a D-glucosamine residue to the C terminal of a phenylalanine residue. The

resultant compounds were termed *1A*, *1T*, *1G*, and *1C*, respectively. Another series of compounds with two phenylalanine residues were also synthesized and they were termed *2A*, *2T*, *2G*, *2C*. All compounds synthesized, except compound 1C, exhibited good gelation properties.

The importance of nucleobases in determining the gelation ability and properties of the hydrogelators was demonstrated in the following few observations. Firstly, it was observed that hydrogelators with different nucleobases gelate under different experimental conditions. For instance, hydrogelators with adenine, cytosine, and guanine contain amine functional groups, which can be protonated under acidic condition. Increasing the pH of solutions with these pre-dissolved hydrogelators triggered gelation. Conversely, hydrogelators with thymine do not possess amine functional groups. They were first dissolved in water at pH 10, and gelation was initiated when the solution pH dropped to around 7. Secondly, the hydrogels formed with different hydrogelators had different physical appearances. Some, like compound 1C, was unable to gelate, while others formed opaque, semitransparent, or transparent gels. Transmission electron microscopy revealed different supramolecular structures, ranging from thin and straight nanofibers to nanoparticles of varying diameter and length. The differences in the gels' optical and microscopic appearance indicate the existence of different self-assembly mechanisms for the various hydrogelators attached to different nucleobases. Thirdly, replacing nucleobase with naphthalene failed to initiate gelation, indicating the importance of nucleobase in forming the three-dimensional network required for gel formation. Fourthly, gels formed with different hydrogelators possessed varying rheological properties, with compound 2C and 1A gel having the highest and lowest storage modulus respectively. Fifthly, the inclusion of nucleobases confers on the hydrogelators the ability to interact with complementary nucleotide sequences. The addition of oligomeric deoxyadenosine to compound 1T led to the formation of a more stable hydrogel with a higher storage modulus, suggesting the presence of additional interbase interactions between complementary adenine and thymine base pairs. Circular dichroism study further revealed enhanced base stacking between oligomeric deoxyadenonine and compound 1T.

This interbase interaction enables the hydrogelators to bind to oligonucleotides and facilitates their delivery into living cells. An experiment involving the delivery of fluorescein-labeled single-stranded oligomeric deoxyadenosine into HeLa cells with the use of 1T was conducted. Green fluorescence was observed in both cell cytosols and nuclei after 24 hours of incubation. In contrast, no fluorescence was detected in the negative control without 1T. Furthermore, replacing 1T with 1G or 1A also led to delivery failure. The ability of the hydrogelators to establish interbase interactions with complementary nucleotide sequences opens up the possibility for such nucleobase-containing hydrogelators to serve as a novel targeted oligonucleotide or gene delivery system.

The same group have also produced another type of nucleopeptide hydrogelator by joining a phenylalanine dipeptide with either one of the four major nucleobases, forming the compounds 1A, 1T, 1G, 1C [81]. Further conjugation of compound 1 with tyrosine phosphate yields compound 2, and compound 3

is formed by subsequent catalytic dephosphorylation of 2. Both compounds 1 and 3 were found to gelate solvents at 2 wt% and at pH 5–7. Incorporation of nucleobases was shown to have a protective effect on the dipeptide. Biostability analysis with proteinase K demonstrated that the presence of nucleobases offers the peptides certain degrees of resistance to enzymatic digestion, suggesting nucleobase incorporation to be an effective approach for improving the biostability of peptide-based hydrogelators *in vitro* and *in vivo*. Aside from biostability, the biocompatibility of these nucleopeptides was also investigated. Cell viabilities were maintained at near 100%, indicating the absence of detrimental cellular damage. A simple wound-healing assay, as seen in Figure 4.9, was also conducted to investigate the ability of the hydrogelators to maintain cell–matrix interaction. The lack of inhibitory effect on cell migration, coupled with the high cell viabilities shown in the *in vitro* cytotoxic study, suggest promising potential for such a hydrogel system to be used as a cell culturing platform in tissue engineering.

Other than peptides, nucleobases or nucleosides can also be incorporated into lipid-based gelators. A glycosyl–nucleoside lipid LMWG synthesized by Godeau *et al*. with double-click chemistry were found to be capable of self-assembling spontaneously into supramolecular structures that gel both water and chloroform [82]. This gelator consisted of a lipidic chain, a thymidine, and a β-D-glucopyranoside, covalently linked together by 1,2,3-triazole bridges. The presence of thymidine is essential for gel formation as an analog without the nucleoside segment was unable to gelate water. The importance of nucleosides in stabilizing the gel's supramolecular structural network was indicated by the lower ultra-violet epsilon values observed, which suggested the occurrence of $\pi-\pi$ stacking events between the nucleosides. In addition to the presence of nucleosides, the gelation property of this glycosyl-nucleoside lipid also depends on the nature of the lipid part and the types of chemical linkage present in the molecule.

Nucleobase incorporation offers additional control over the mode of supramolecular self-assembly of steroids. Typically, a steroid gel comprises multiple mesogenic units, stacked in a helical and columnar fashion to form a central core, with functional groups substituted at the steroid C3 position sticking outward, resembling a spiral staircase. Introduction of uracil to C3 by Snip *et al*. led to the discovery of an excellent gelator [83]. Higher gel stability, as indicated by a lower sol–gel transition temperature, was obtained with the uracil-substituted steroid as compared to an analog connected to a uracil moiety with its NH group substituted with a methyl, suggesting the role of inter-gelator hydrogen bonding, in addition to aromatic stacking between extended steroid planes, in stabilizing the organogel. The stability and morphology of the organogel can be altered by the addition of polynucleotides [84]. A mixture of polynucleotides with uracil-substituted steroids was found to possess higher gelation ability. Interestingly, the mixture of polyadenylic acid with steroid formed a well-developed tape-like fibrous network twisted in a right-angle fashion, while the mixture of polycytidylic acid with steroid produced only a fibrous network with no helical structure. This observation demonstrated the effects of complementary interbase

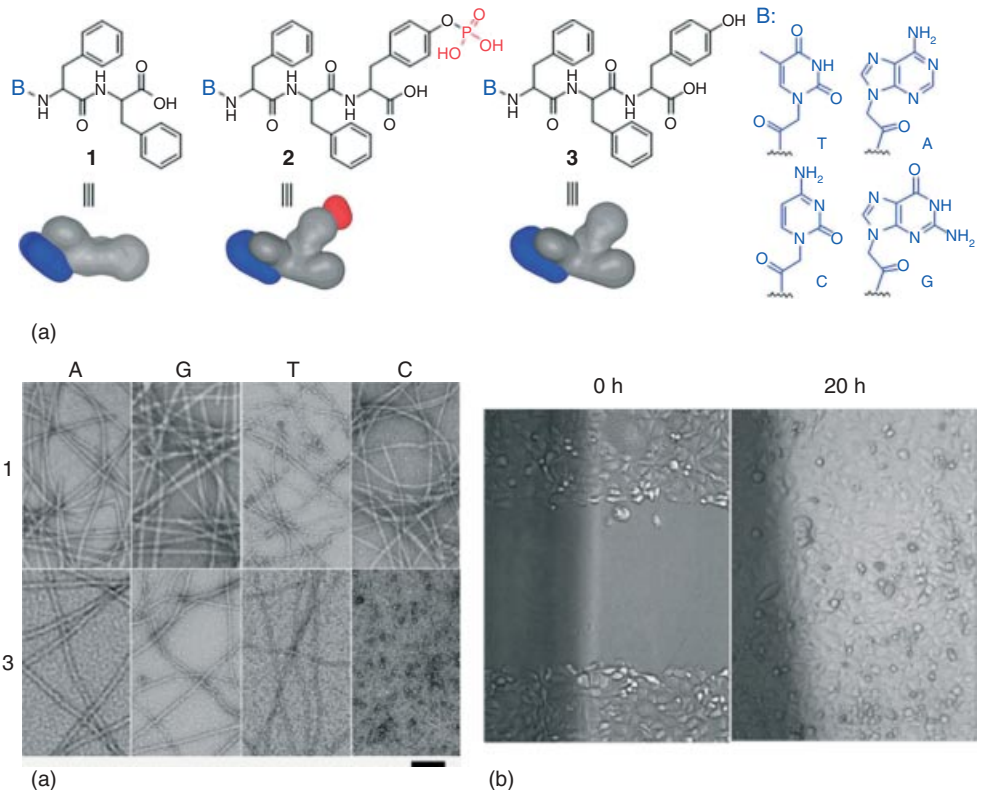

Figure 4.9 (A) Molecular structures and shapes of the nucleopeptidehydrogelators and their corresponding precursors. (B) TEM micrographs of the hydrogels formed by nucleopeptides 1A, 1G, 1T, 1C, 3A, 3G, 3T and the solution of 3C; Scale bar = 100 nm. (C) Result of a simple wound healing assay represented by optical images of HeLa cells on the surface 0 and 20 hours after creation of scratches in the presence of hydrogelator 3T. (Figure adapted from Ref. [81] (Copyright 2011) John Wiley & Sons, Inc.)

hydrogen bonding on the packing and morphology of the gel's self-assembled structures.

4.4.4.2 **Nucleic Acid Chains**

Nucleic acids are polymerized nucleotides, existing usually as double-stranded structures, with each strand carrying a nucleotide sequence complementary to the other, linked together by inter-base pairs hydrogen bonding. Even though the molecular weight of nucleic acids may be considerably larger than the arbitrary limit of 3000 Da set forth by some literature, they are still included here, owing to their inherent biocompatibility, the ability to self-associate via non-covalent interactions, the ease of breaking down the resultant gels, the ability to design specific nucleotide sequences to alter gelation properties, and their diverse and promising potential in the field of biomedical research.

Double-stranded nucleic acids with single-stranded overhangs have demonstrated gelating potential. Cheng *et al*. have produced a fast and pH-responsive gel with three-armed double-stranded deoxyribonucleic acid (DNA) nanostructures [85]. The gelator, which was termed as the *Y unit*, is comprised of three 37mer single stranded DNAs. Of the 37 nucleotides, 11 represent the interlocking motif domain with 2 cytosine-rich stretches that can be cross-linked to another Y unit. The remaining 26 nucleotides contain 2 half-complementary sequences that are essential for the formation of the double-stranded Y shape of the Y unit. Gelation is evoked by low pH, which encourages the formation of intermolecular interlocking motif structures. Interlocking domains that were initially separated by electronic repulsion would be partially protonated upon the addition of hydrochloric acid. Protonated cytosine residues in the interlocking domain would then form hydrogen bonds with unprotonated cytosine residues, forming the interlocking motifs that link different Y units together and form extended interconnected networks.

One important characteristic of this hydrogel is that it is sensitive to pH changes. To demonstrate this ability, the authors have incorporated water-soluble citrate-modified 13 nm gold nanoparticles into the hydrogel. The results, as shown in Figure 4.10, showed that no nanoparticles were released for several days after the hydrogel was formed. The addition of sodium hydroxide, however, resulted in rapid release of the entrapped nanoparticles within minutes, suggesting that the hydrogel is capable of encapsulating small substances with high efficiency and stability and that the gel can be easily reverted back to its solution state by changing the environmental pH. In addition, the authors have shown that the hydrogel stability can be affected by temperature; in particular, the gelling transition temperature of the DNA hydrogel formed was found to be at 37 °C at a gelator concentration of 0.6 mM. This pH- and temperature-sensitive DNA hydrogel possesses tremendous potential in the field of controlled release, where chemicals or biologics can be incorporated in and released from the hydrogel by responding to local changes in pH and temperature specific to diseased tissues. While the molecular weights of the DNA gelators used in the above study have exceeded the limit of 3000 Da, it is worth noting that this hydrogel still shares many characteristics with classical molecular gels, for example, gelation which is achieved by self-assembly of individual monomers via non-covalent interactions and the relative ease of breaking down the gels formed by simply changing the environmental pH.

In addition to hydrogen bonding as a means of forming DNA hydrogel, it can also be formed by cross-linking nucleic acids via phosphodiester bonds with DNA ligase. Such double-stranded DNAs usually possess single-stranded palindromic end sequences that permit hybridization with complementary sequences. Technically, this type of DNA hydrogels would not fit the strict definition of molecular gel because of the high molecular weight of the gelators used and the covalent nature of the bonds that form the gelation network. However, this type of DNA hydrogels differs significantly from the other types of chemically cross-linked hydrogels, for which no potentially harmful chemicals are needed to trigger the gelation process and the gels formed can be broken down easily with the use of DNA

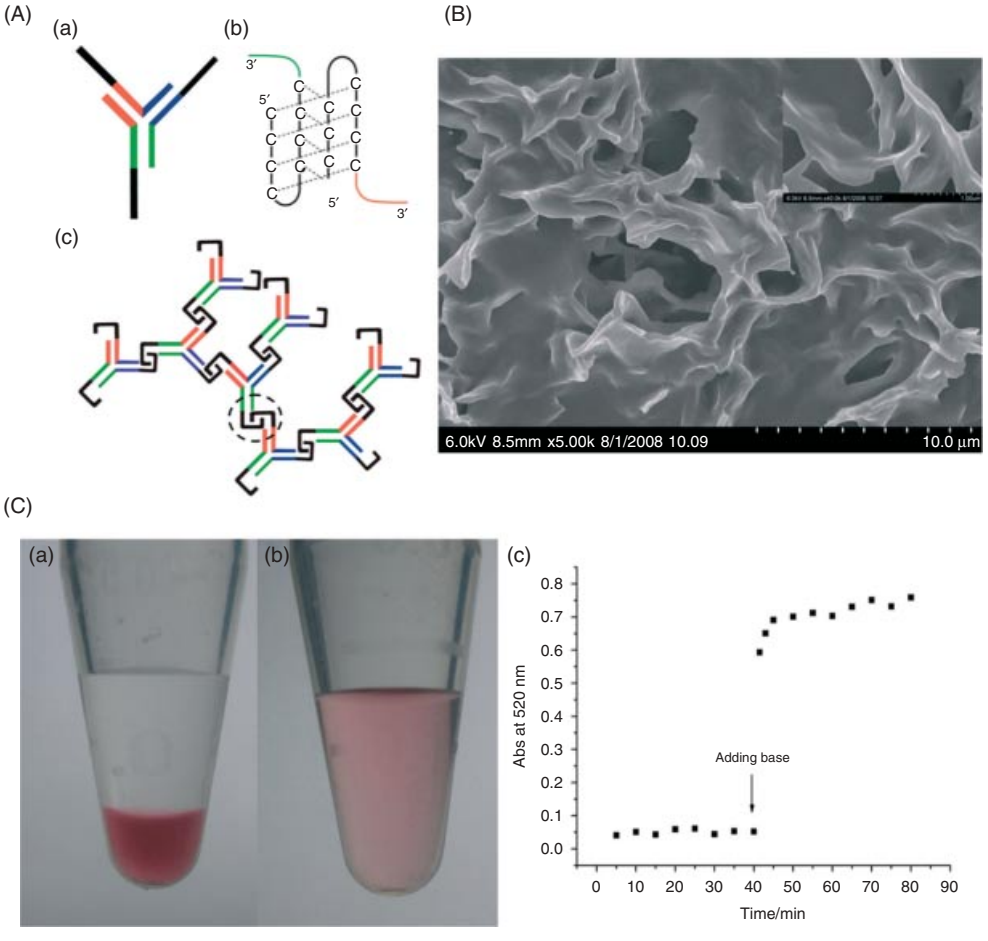

Figure 4.10 (A) Structure of the pH-responsive DNA gel. (a) A Y-shaped DNA nanostructure with three free interlocking domains, also known as the *Y unit*. (b) Enlarged image of the circled region demonstrating the formation of inter-Y-unit I motif. (c) DNA hydrogel made from the three-dimensional assemble of Y units. The sequences of the 3 DNA strands used in the Y units, coded with different colors according to different domains, are: (a) 5′-CCCCTAACCCCTGGATCCGCATGACATTCG CCGTAAG-3′; (b) 5′-CCCCTAACCCCCTTACG-GCGAATGACCGAATCAGCCT-3′; and (c) 5′-CCCCTAACCCCAGGCTGATTCGGTTCATG CGGATCCA-3′. (B) FE-SEM image of the dried DNA hydrogel showing its fine lamellar structure (C) Gel transition triggered by pH changes (a) 7 nm water-soluble citrate-modified 13 nm gold nanoparticles (GNPs) as tracer agent were trapped in DNA hydrogel with a layer of MES buffer at pH 5.0. (b) GNPS were released from the DNA hydrogel and form a uniformly colored solution upon the addition of NaOH, which increased the pH value of the buffer to 8.0. (c) Time trace of the absorption at 520 nm for the upper part of the solution before and after addition of NaOH. (Figure adapted from Ref. [85] (Copyright 2009) John Wiley & Sons, Inc.)

nucleases. Furthermore, compared to other synthetic polymers like poly(lactic acid) or polyethylene glycol, there will be fewer issues associated with biocompatibility as DNAs are present naturally in the human body.

The ability to engineer and design specific sequences on the DNA gelators further expanded the usage of chemically cross-linked DNA hydrogels in a variety of research fields, including tissue engineering. Due to their diverse applications in the medical and pharmaceutical industries and their unique characteristic of being able to be disintegrated easily, a property that is shared with the molecular gels, enzymatically cross-linked DNA hydrogels therefore warrant the attention of this review.

Um *et al*. have devised an enzyme-catalyzed assembly of large scale three-dimensional DNA hydrogel with branched DNAs of varying shapes [86]. Branched DNAs in the shapes of T, Y, and X have all demonstrated the ability to gelate solvents with the aid of DNA T4 ligase. The gels formed from different branched DNA molecules at various concentrations possessed significantly different physical and mechanical properties. For instance, X-DNA hydrogel had the strongest tensile modulus and the lowest tensile strength compared to Y-DNA and T-DNA hydrogels. Morphology observation revealed different internal structures for different hydrogels, with X-DNA gel comprising two flat stripes tangled into a knot, Y-DNA gels having branched fibers, and X-DNA possessing puckers-like scales. Further visualization revealed that X-DNA gel contained standardized and well-controlled nanoscale holes of 12.3 ± 1.3 nm, which were absent in both Y-DNA and T-DNA hydrogels. In addition to varying physical and mechanical properties, the hydrogels formed also differed in terms of their biodegradability. Daily DNA mass loss analysis indicated that X-DNA hydrogel had the slowest degradation rate over a period of two weeks. Loading the gels with DNA-binding chemical entities like camptothecin was shown to confer a protective effect on the gel by prolonging their degradation. To investigate the drug delivery potentials of the hydrogels, insulin was loaded into the gels and its release profile was determined. Insulin was released in a slow and sustained manner, with those loaded into the X-DNA hydrogels having the slowest rate of release, which coincided with the slow degradation rate demonstrated by the X-DNA hydrogels.

The use of DNA ligase in catalyzing the gelation process eliminated the need for organic solvents, extreme pH, high temperature, and long reaction time. This allowed for increased efficiency and decreased cytotoxicity in live mammalian cells encapsulation, and, in this paper, CHO cells incorporated *in situ* into the X-DNA hydrogels were able to remain viable after three days of incubation, as demonstrated in Figure 4.11. The positive result of this cell study exhibited not only the DNA hydrogels' biocompatibility, but also their promising potential to be used in tissue engineering as three-dimensional cell culture platforms. The ability to disintegrate and to digest DNA gels with nucleases enables possible cell retrieval after cell culture, further reinforcing their usefulness in tissue engineering.

In another report, Park *et al*. have successfully fabricated a cell-free protein-producing gel that can produce proteins 300 times more efficiently than existing solution processes [87]. Ligation of the gene of interest, in this case the *renilla luciferase* gene, with X-DNA connectors by DNA ligase yielded a protein-producing

(A)

Strand	Sequence
X_{01}	5′ -p-ACGT CGA CCG ATG AAT AGC GGT CAG ATC CGT ACC TAC TCG-3′
X_{02}	5′ -p-ACGT CGA GTA GGT ACG GAT CTG CGT ATT GCG AAC GAC TCG-3′
X_{03}	5′ -p-ACGT CGA GTC GTT CGC ATT ACG GCT GTA CGT ATG GTC TCG-3′
X_{04}	5′ -p-ACGT CGA GAC CAT ACG TAC AGC ACC GCT ATT CAT CGG TCG-3′
Y_{01}	5′ -p-ACGT CGA CCG ATG AAT AGC GGT CAG ATC CGT ACC TAC TCG-3′
Y_{02}	5′ -p-ACGT CGA GTC GTT CGC AAT ACG ACC GCT ATT CAT CGG TCG-3′
Y_{03}	5′ -p-ACGT CGA GTA GGT ACG GAT CTG CGT ATT GCG AAC GAC TCG-3′
T_{01}	5′ -p-ACGT CGA CAG CTG ACT AGA GTC ACG ACC TGT ACC TAC TCG-3′
T_{02}	5′ -p-ACGT CGA GTC GTT CTC AAG ACG TAG CTA GGA CTC TAG TCA GCT GTC G-3′
T_{03}	5′ -p-ACGT CGA GTA GGT ACA GGT CGT CGT CTT GAG AAC GAC TCG-3′

p represents the phosphorylation on the 5′ end of the oligonucleotide

(B)

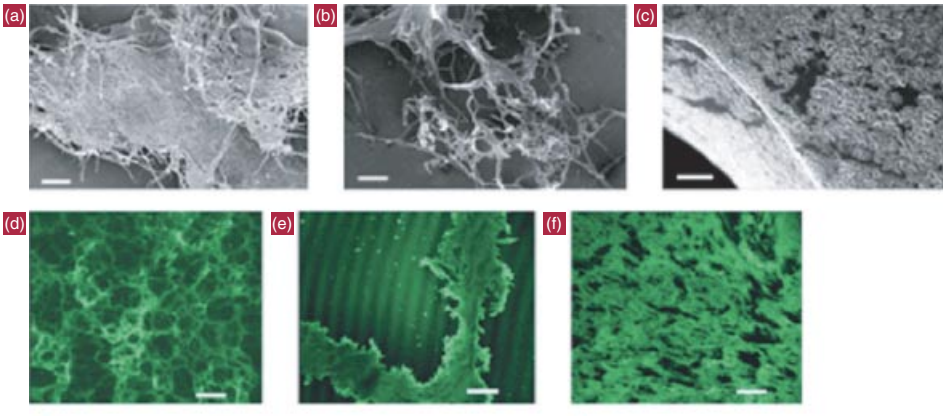

(C)

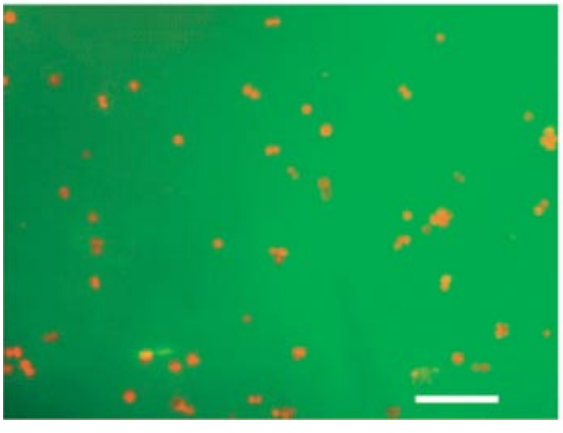

gel (P-gel). Protein expression was achieved by incubating P-gel with wheat germ lysates, consisting of RNA polymerase and ribosomes, for 24 h. The amount and functionality of the proteins produced by the P-gels were analyzed, quantified, and compared with those proteins synthesized from commercially available cell-free solution-based protein expression systems. It was revealed that P-gel was able to produce up to 5 mg mL^{-1} of functional proteins, a number that is significantly higher than the levels achievable by conventional solution processes, at a faster rate and for a longer duration.

The high yield and efficiency of protein expression were hypothesized to be due to the following reasons. Firstly, the stability of the protein genomic information is enhanced due to the protective effect conferred by covalently cross-linked X-DNA linkers that make the gene less susceptible to enzymatic and hydrolytic degradation. Secondly, there is an increase in overall gene concentration in a gel phase compared with that in a solution phase, which possesses additional solvent volume. Thirdly, an elevation in the turnover rate of the biosynthetic machinery is apparent as a result of closer gene proximity within a gel structure. Lastly, high abundance of bivalent cations inside the hydrogel matrix, due to the presence of polyanionic DNA, enhances the activity of transcription machineries by mimicking the condensed phase of chromatin in a normal cell nucleus with high ionic concentration [88].

In addition to *renilla luciferase*, 16 other functional proteins, including membrane proteins, receptor proteins, and even toxic proteins, have been synthesized by altering the gene sequences incorporated into the P-gels, with similar high yield and efficiency. This highlighted the highly flexible and adaptable nature of P-gel to produce a wide variety of complex proteins and even toxic proteins that cannot be otherwise synthesized using a cell-based system, suggesting its potential application in the field of onsite protein production and high-throughput protein engineering.

4.5 Summary

Here we focus on the recent strategies in designing biomaterials into molecular gels and their present and potential applications in tissue engineering. Compared to polymer-based hydrogels, which do not usually degrade under physiological

Figure 4.11 (A) Oligonucleotide sequences of the DNA building blocks for the DNA hydrogels. (B) External morphologies and internal structures of different DNA hydrogels; FE-SEM images of dried X-DNA (a), T-DNA (b), and T-DNA (c) hydrogels; Confocal microscopic images of the swollen X-DNA (d), Y-DNA (e), and T-DNA (f) hydrogels; The scale bars are 200 µm for (a,d,f), 50 µm for (b), 15 µm for (c), and 10 µm for (e). (C) Fluorescent images of live CHO cells encapsulated into a X-DNA hydrogel. CHO cells were stained red by CellTrackerTM Red CMTPX Probes while the DNA hydrogel was stained green with SYBR I dye. Scale bar = 100 µm. (Figure adapted from Ref. [86] (Copyright 2006) Nature Publishing Group.)

conditions, molecular gels have outstanding bio-degradability. For example, molecular gels containing cells for tissue regeneration can be designed to promote cell growth initially, and then gradually degrade in a controlled manner by enzymatic hydrolysis, so as to not interfere with cell differentiation at a later stage. In addition, self-assembly makes molecular gels clear of toxicity caused by cross-linking initiation. The defined control over the physical and chemical properties of a molecular gel for specific applications is another advantage. Peptide amphiphile is an example of refined control over molecular gel gelation by altering and designing the molecular structure of the gelators. The serendipity of the identification of gelators has developed into syntheses and applications of a variety of peptides for tissue regeneration. In contrast to natural polymer-based hydrogels such as collagen and gelatin, the applications of saccharide-based molecular gel in tissue engineering are only beginning to be realized, with huge potentials. While the use of lipid-based molecular gels is still generally limited to targeted drug delivery at the present time, some promising potentials for them to support cell growth and adhesion have been successfully demonstrated. Nucleic acid and nucleobases containing molecular gels, aside from tissue engineering, have also demonstrated other new and exciting biomedical applications, such as cell-free protein expression and controlled drug delivery. However, notwithstanding all the desirable properties that molecular gels possess for the future of patient-tailored tissue engineering, they are still restricted by the lack of suitable mechanical properties and the inability to produce a mechanically dynamic environment of the kind that many tissues are living in, and these pose challenges for future improvements to address.

List of Abbreviations

CAB	3-β-cholesteryl-4-(2-anthryl)butanoate
$DC_{8,9}PC$	Diacetylene-1,2-bis(tricosa-10,12-diynoyl)-sn-glycero-3-phosphocholine
EAK	16 Glutamic acid-alanine-lysine 16
ECM	Extracellular matrix
GP-1	*N*-lauroyl-L-glutamic acid di-*n*-butylamide
HAS 12-	Hydroxystearic acid
IKVAV	Isoleucine-lysine-valine-alanine-valine
LMWGs	Low-molecular-weight gelators
MSC	Mesenchymal stem cells
MTT	3-(4,5-Dimethylthiazol-2-yl)-2,5-diphenyltetrazolium bromide
P-gel	Protein-producing gel
PS	Phosphatidylserine
RAD	Arginine-alanine-aspartic acid
RGD	Arginine-glycine-aspartic acid
SAPNS	Self-assembling peptide nano-fiber scaffold
S1P	Sphingosine-1-phosphate

Appendix: Gelators and their Potential Use and Applications

Class	Gelators	Estimated molecular weight	Potential use and application
Amphiphilic peptides	RAD 16 or ARADADARARADADA [15] EAK 16: AEAEAKAKAEAEAKAK [15]	RAD 16: 1515.58 EAK16: 1615.81	Assemble into a stable and macroscopic membranous matrix for cell adhesion when transferred into physiological solutions. Cell lines capable of attaching to the matrix • NIH-3T3(Mouse fibroblast) • CEF(Chick embryo fibroblast) • CHO(Chinese hamster ovary) • MG63 (Human osteosarcoma cell line) • HepG2 (Hepatocellular carcinoma cell line) • HIT-T15 (hamster insulinoma tumor T15) • HEK293 (Human embryonic kidney 293 cells) • SH-SY5Y (human neuroblastoma cell line) • PC12(Rat pheochromocytoma)
Amphiphilic peptides	RAD 16 I: RADARADARADARADA-I [33] RAD 16 II: RARADADARARADADA-II [33]	RAD 16-I: 1671.77 RAD 16-II: 1671.77	Promote neurite outgrowth, synapse formations, and axon regeneration.
Amphiphilic peptides	KLD-12 or KLDLKLDLKLDL-12 [43]	1426.75	Cartilage tissue regeneration
Peptide amphiphiles	IKVAV-Peptide amphiphiles [37]	528.68	Directed neural progenitor cells differentiation into neurons but not astrocytes
Peptide amphiphiles	Heparin-binding peptide amphiphile LRKKLGKA-PA [46, 47]	913.16	Blood vessel formation and islet transplantation
Saccharides	A glycosylated amino acetate type of hydrogelator 1 $C_{33}O_{12}N_3H_{55}$ [10]	685.00	Discrimination of phosphate derivatives
Saccharides	Gelator 4b (a derivative of D-gluconolactone) $C_{16}O_7N_2H_{24}$ [47]	356.00	Detection of trace insulin
Saccharides	glyco-lipid 1 (muconic amide as the spacer and GlcNAc (*N*-acetyl glucosamine) as the head) $C_{35}O_{12}N_3H_{55}$ [48]	709.00	Encapsulation and distribution of live Jurkat cells

(continued overleaf)

(*continued*)

Class	Gelators	Estimated molecular weight	Potential use and application
Lipid	Equimolar mixture of 1,2-bis(10,12-tricosadiynoyl)-*sn*-glycero-3-phosphocholine and 1,2-bis(dinonanoyl)-*sn*-glycero-3-phosphocholine [59]	914.28 and 537.67 respectively	Encapsulation and release of growth factors for nerve regeneration and osteogenic differentiation. High water content and biocompatible hydrogels formed possess potential to be used in tissue engineering
Lipid	12-hydroxystearic acid [5]	300.48	CHO cells remained viable and attached for at least 21 days on the microporous organogel scaffolds. Possible collagen production observed
Nucleobase	Guanosine derivatives [79]	151.13	
Nucleobase-containing hybrid	Nucleobase–amino acid–glycosides hybrid (nucleobase, phenylalanine, D-glucosamine) [80]	1T: 492.00 1C: 477.00 (non-gelator) 1A: 501.00 1G: 517.00 2T: 639.00 2C: 624.00 2A: 648.00 2G: 664.00 * T, C, A, G represent thymine, cytosine, adenine, guanine respectively	Delivery of fluorescein-labeled single-stranded oligomeric deoxyadenonine into HeLa cells
Nucleobase-containing hybrid	Nucleopeptide (phenylalanine dipeptide link to a nucleobase) [81]	1T: 478.00 1C: 463.00 1A: 487.00 1G: 505.00 3T: 641.00 3C: 626.00 (non-gelator) 3A: 650.00 3G: 666.00 * T, C, A, G represent thymine, cytosine, adenine, guanine respectively	Near 100% HeLa cell viability upon incubation with hydrogelators for 72 h, indicating absence of significant cytotoxicity. Little inhibitory effect by hydrogelators on cell migration

(*continued*)

Class	Gelators	Estimated molecular weight	Potential use and application
Nucleoside-containing hybrid	Glycosyl-nucleoside lipid (lipidic chain, thymidine, and β-D-glucopyranoside) [82]	5a: 829.00 5b: 831.00 5c: 818.00 5d: 934.00 * a, b, c, d represent different lipidic chain segments	Enhance gelation
Nucleobase-containing hybrid	Uracil to C3 of a steroid [83]	629.00	Enhance gelation and alter mode of self-assembly
Nucleic acid chains	Three-armed double-stranded DNA nanostructures (Y-unit) with cytosine-rich stretches that could be cross-linked via hydrogen bonding [85]	33947.70	pH- and temperature-sensitive controlled release of chemicals and biologics
Nucleic acid chains	Branched DNA in the shapes of T, Y, and X linked by DNA ligase [86]	T-DNA: 38806.90 Y-DNA: 35581.00 X-DNA: 48908.00	Encapsulation and release of insulin. CHO cells encapsulated *in situ* remained viable after three days of incubation in hydrogel. Possible to retrieve cultured cells by disintegrating DNA hydrogels with nucleases
Nucleic acid chains	Ligation of protein gene with X-DNA connectors with DNA ligase [87]	X-DNA connectors: 48908.00 Variable length for linear plasmids encoding for protein of interest.	Cell-free protein expression with high yield and efficiency.

References

1. Ferry, J. (1980) *Viscoelastic Properties of Polymers*, 3rd edn, John Wiley & Sons, Inc., New York.
2. Terech, P. and Weiss, R.G. (1997) *Chem. Rev.*, **97**, 3133–3160.
3. Steed, J.W. (2011) *Chem. Commun. (Camb.)*, **47**, 1379–1383.
4. Kang, L., Liu, X.Y., Sawant, P.D., Ho, P.C., Chan, Y.W., and Chan, S.Y. (2005) *J. Controlled Release*, **106**, 88–98.
5. Lukyanova, L., Franceschi-Messant, S., Vicendo, P., Perez, E., Rico-Lattes, I., and Weinkamer, R. (2010) *Colloids Surf., B*, **79**, 105–112.
6. Sangeetha, N.M. and Maitra, U. (2005) *Chem. Soc. Rev.*, **34**, 821–836.

7. Smith, A.D. (2008) in *Organic Nanostructures* (eds J.L. Atwood and J.W. Steed), Wiley-VCH Veralg GmbH, Weinheim, pp. xviii–352.
8. Smith, D.K., Hirst, A.R., Escuder, B., and Miravet, J.F. (2008) *Angew. Chem. Int. Ed.*, **47**, 8002–8018.
9. Dastidar, P. (2008) *Chem. Soc. Rev.*, **37**, 2699–2715.
10. Hamilton, A.D. and Estroff, L.A. (2004) *Chem. Rev.*, **104**, 1201–1217.
11. Miyata, T., Asami, N., and Uragami, T. (1999) *Nature*, **399**, 766–769.
12. Yamaguchi, S., Yoshimura, I., Kohira, T., Tamaru, S., and Hamachi, I. (2005) *J. Am. Chem. Soc.*, **127**, 11835–11841.
13. Fenniri, H., Mathivanan, P., Vidale, K.L., Sherman, D.M., Hallenga, K., Wood, K.V., and Stowell, J.G. (2001) *J. Am. Chem. Soc.*, **123**, 3854–3855.
14. Fuhrhop, J.H. and Helfrich, W. (1993) *Chem. Rev.*, **93**, 1565–1582.
15. Brunsveld, L., Folmer, B.J., Meijer, E.W., and Sijbesma, R.P. (2001) *Chem. Rev.*, **101**, 4071–4098.
16. Aggeli, A., Nyrkova, I.A., Bell, M., Harding, R., Carrick, L., McLeish, T.C., Semenov, A.N., and Boden, N. (2001) *Proc. Natl. Acad. Sci. U.S.A.*, **98**, 11857–11862.
17. Zhang, S., Holmes, T.C., DiPersio, C.M., Hynes, R.O., Su, X., and Rich, A. (1995) *Biomaterials*, **16**, 1385–1393.
18. Kiyonaka, S., Sada, K., Yoshimura, I., Shinkai, S., Kato, N., and Hamachi, I. (2004) *Nat. Mater.*, **3**, 58–64.
19. Elisseeff, J., McIntosh, W., Anseth, K., Riley, S., Ragan, P., and Langer, R. (2000) *J. Biomed. Mater. Res.*, **51**, 164–171.
20. Liu Tsang, V., Chen, A.A., Cho, L.M., Jadin, K.D., Sah, R.L., DeLong, S., West, J.L., and Bhatia, S.N. (2007) *FASEB J.*, **21**, 790–801.
21. Weber, L.M., Hayda, K.N., Haskins, K., and Anseth, K.S. (2007) *Biomaterials*, **28**, 3004–3011.
22. Kang, L., Hancock, M.J., Brigham, M.D., and Khademhosseini, A. (2010) *J. Biomed. Mater. Res. A*, **93**, 547–557.
23. LeRoux, M.A., Guilak, F., and Setton, L.A. (1999) *J. Biomed. Mater. Res.*, **47**, 46–53.
24. Cui, H., Webber, M.J., and Stupp, S.I. (2010) *Biopolymers*, **94**, 1–18.
25. Wang, R., Liu, X.-Y., Xiong, J., and Li, J. (2006) *J. Phys. Chem. B*, **110**, 7275–7280.
26. Li, J.-L., Liu, X.Y., Strom, C.S., and Xiong, J.Y. (2006) *Adv. Mater.*, **18**, 2754–2758.
27. Tang, S., Liu, X.Y., and Strom, C.S. (2009) *Adv. Funct. Mater.*, **19**, 2252–2259.
28. Li, J.-L., Yuan, B., Liu, X.-Y., Wang, X.-G., and Wang, R.-Y. (2011) *Cryst. Growth Des.*, **11**, 3227–3234.
29. Li, J.-L. and Liu, X.-Y. (2009) *J. Phys. Chem. B*, **113**, 15467–15472.
30. Dawn, A., Shiraki, T., Haraguchi, S., Tamaru, S., and Shinkai, S. (2011) *Chem. Asian J.*, **6**, 266–282.
31. Nuttelman, C.R., Benoit, D.S., Tripodi, M.C., and Anseth, K.S. (2006) *Biomaterials*, **27**, 1377–1386.
32. Smith, A.D. (2008) Molecular gels, in *Organic Nanostructures*, 1st edn (eds J.L. Atwood and J.W. Steed), Wiley-VCH Verlag GmbH, Weinheim.
33. Holmes, T.C., de Lacalle, S., Su, X., Liu, G., Rich, A., and Zhang, S. (2000) *Proc. Natl. Acad. Sci. U.S.A.*, **97**, 6728–6733.
34. Ellis-Behnke, R.G., Liang, Y.X., You, S.W., Tay, D.K., Zhang, S., So, K.F., and Schneider, G.E. (2006) *Proc. Natl. Acad. Sci. U.S.A.*, **103**, 5054–5059.
35. Wang, C., Varshney, R.R., and Wang, D.A. (2010) *Adv. Drug Delivery Rev.*, **62**, 699–710.
36. Harrington, D.A., Cheng, E.Y., Guler, M.O., Lee, L.K., Donovan, J.L., Claussen, R.C., and Stupp, S.I. (2006) *J. Biomed. Mater. Res. A*, **78**, 157–167.
37. Silva, G.A., Czeisler, C., Niece, K.L., Beniash, E., Harrington, D.A., Kessler, J.A., and Stupp, S.I. (2004) *Science*, **303**, 1352–1355.
38. Niece, K.L., Czeisler, C., Sahni, V., Tysseling-Mattiace, V., Pashuck, E.T., Kessler, J.A., and Stupp, S.I. (2008) *Biomaterials*, **29**, 4501–4509.
39. Zhang, S., Holmes, T., Lockshin, C., and Rich, A. (1993) *Proc. Natl. Acad. Sci. U.S.A.*, **90**, 3334–3338.
40. Freed, L.E., Marquis, J.C., Nohria, A., Emmanual, J., Mikos, A.G., and Langer, R. (1993) *J. Biomed. Mater. Res.*, **27**, 11–23.

41. Semino, C.E., Merok, J.R., Crane, G.G., Panagiotakos, G., and Zhang, S. (2003) *Differentiation*, **71**, 262–270.
42. Lemare, F., Steimberg, N., Le Griel, C., Demignot, S., and Adolphe, M. (1998) *J. Cell. Physiol.*, **176**, 303–313.
43. Kisiday, J., Jin, M., Kurz, B., Hung, H., Semino, C., Zhang, S., and Grodzinsky, A.J. (2002) *Proc. Natl. Acad. Sci. U.S.A.*, **99**, 9996–10001.
44. Storrie, H., Guler, M.O., Abu-Amara, S.N., Volberg, T., Rao, M., Geiger, B., and Stupp, S.I. (2007) *Biomaterials*, **28**, 4608–4618.
45. Paramonov, S.E., Jun, H.W., and Hartgerink, J.D. (2006) *J. Am. Chem. Soc.*, **128**, 7291–7298.
46. Rajangam, K., Behanna, H.A., Hui, M.J., Han, X., Hulvat, J.F., Lomasney, J.W., and Stupp, S.I. (2006) *Nano Lett.*, **6**, 2086–2090.
47. Stendahl, J.C., Wang, L.J., Chow, L.W., Kaufman, D.B., and Stupp, S.I. (2008) *Transplantation*, **86**, 478–481.
48. Yoza, K., Ono, Y., Yoshihara, K., Akao, T., Shinmori, H., Takeuchi, M., Shinkai, S., and Reinhoudt, D.N. (1998) *Chem. Commun.*, 907–908.
49. Yoza, K., Amanokura, N., Ono, Y., Akao, T., Shinmori, H., Takeuchi, M., Shinkai, S., and Reinhoudt, D.N. (1999) *Chem. — Eur. J.*, **5**, 2722–2729.
50. Ostuni, E., Kamaras, P., and Weiss, R.G. (1996) *Angew. Chem., Int. Ed. Engl.*, **35**, 1324–1326.
51. Lin, Y.C., Kachar, B., and Weiss, R.G. (1989) *J. Am. Chem. Soc.*, **111**, 5542–5551.
52. Furman, I. and Weiss, R.G. (1993) *Langmuir*, **9**, 2084–2088.
53. Terech, P., Furman, I., and Weiss, R.G. (1995) *J. Phys. Chem.*, **99**, 9558–9566.
54. Kiyonaka, S., Shinkai, S., and Hamachi, I. (2003) *Chemistry*, **9**, 976–983.
55. Bhuniya, S. and Kim, B.H. (2006) *Chem. Commun. (Camb.)*, 1842–1844.
56. Hamachi, I., Ikeda, M., Ueno, S., Matsumoto, S., Shimizu, Y., Komatsu, H., and Kusumoto, K.I. (2008) *Chem. — Eur. J.*, **14**, 10808–10815.
57. John, G., Masuda, M., Okada, Y., Yase, K., and Shimizu, T. (2001) *Adv. Mater.*, **13**, 715–718.
58. Fahy, E., Subramaniam, S., Murphy, R. C., Nishijima, M., Raetz, C. R., Shimizu, T., Spener, F., van Meer, G., Wakelam, M. J., and Dennis, E. A. (2009) *J. Lipid Res.* **50** (Suppl.), S9–S14.
59. Collier, J.H. and Messersmith, P.B. (2001) *Annu. Rev. Mater. Res.*, **31**, 237–263.
60. van Etten, E.W., ten Kate, M.T., Stearne, L.E., and Bakker-Woudenberg, I.A. (1995) *Antimicrob. Agents Chemother.*, **39**, 1954–1958.
61. Yager, P. and Schoen, P.E. (1984) *Mol. Cryst. Liq. Cryst.*, **106**, 371–381.
62. Johnson, M.R., Lee, H.J., Bellamkonda, R.V., and Guldberg, R.E. (2009) *Acta Biomater.*, **5**, 23–28.
63. Svenson, S.N. and Messersmith, P.B. (1999) *Langmuir*, **15**, 4464–4471.
64. Yu, X. and Bellamkonda, R.V. (2003) *Tissue Eng.*, **9**, 421–430.
65. Spector, M.S., Singh, A., Messersmith, P.B., and Schnur, J.M. (2001) *Nano Lett.*, **1**, 375–378.
66. Ma, P.X. (2004) *Mater. Today*, **7**, 30–40.
67. Kang, I.K., Ito, Y., Sisido, M., and Imanishi, Y. (1989) *J. Biomed. Mater. Res.*, **23**, 223–239.
68. Wang, R.-Y., Liu, X.-Y., Narayanan, J., Xiong, J.-Y., and Li, J.-L. (2006) *J. Phys. Chem. B*, **110**, 25797–25802.
69. Li, J.-L., Wang, R.-Y., Liu, X.-Y., and Pan, H.-H. (2009) *J. Phys. Chem. B*, **113**, 5011–5015.
70. Ghosh, K., Pan, Z., Guan, E., Ge, S., Liu, Y., Nakamura, T., Ren, X.D., Rafailovich, M., and Clark, R.A. (2007) *Biomaterials*, **28**, 671–679.
71. Avery, K., Avery, S., Shepherd, J., Heath, P.R., and Moore, H. (2008) *Stem Cells Dev.*, **17**, 1195–1205.
72. He, X., H'ng, S.C., Leong, D.T., Hutmacher, D.W., and Melendez, A.J. (2010) *J. Mol. Cell. Biol.*, **2**, 199–208.
73. Zhao, Z.Q., Chen, Z.B., Zhao, X.B., Pan, F., Cai, M.H., Wang, T., Zhang, H.G., Lu, J.R., and Lei, M. (2011) *J. Biomed. Sci.*, **18**, 37.
74. Vance, J.E. and Steenbergen, R. (2005) *Prog. Lipid Res.*, **44**, 207–234.
75. Xu, C.X., Su, P.Q., Chen, X.F., Meng, Y.C., Yu, W.H., Xiang, A.P., and Wang, Y.J. (2011) *Biomaterials*, **32**, 1051–1058.

76. Araki, K. and Yoshikawa, I. (2005) *Top. Curr. Chem.*, **256**, 133–165.

77. Sessler, J.L., Lawrence, C.M., and Jayawickramarajah, J. (2007) *Chem. Soc. Rev.*, **36**, 314–325.

78. Mutai, K., Gruber, B.A., and Leonard, N.J. (1975) *J. Am. Chem. Soc.*, **97**, 4095–4104.

79. Davis, J.T. (2004) *Angew. Chem. Int. Ed.*, **43**, 668–698.

80. Li, X., Yi, K., Shi, J., Gao, Y., Lin, H.C., and Xu, B. (2011) *J. Am. Chem. Soc.*, **133**, 17513–17518.

81. Li, X., Kuang, Y., Lin, H.C., Gao, Y., Shi, J., and Xu, B. (2011) *Angew. Chem. Int. Ed.*, **50**, 9365–9369.

82. Godeau, G. and Barthelemy, P. (2009) *Langmuir*, **25**, 8447–8450.

83. Snip, E., Koumoto, K., and Shinkai, S. (2002) *Tetrahedron*, **58**, 8863–8873.

84. Numata, M., Sugiyasu, K., Kishida, T., Haraguchi, S., Fujita, N., Park, S.M., Yun, Y.J., Kim, B.H., and Shinkai, S. (2008) *Org. Biomol. Chem.*, **6**, 712–718.

85. Cheng, E., Xing, Y., Chen, P., Yang, Y., Sun, Y., Zhou, D., Xu, L., Fan, Q., and Liu, D. (2009) *Angew. Chem. Int. Ed.*, **48**, 7660–7663.

86. Um, S.H., Lee, J.B., Park, N., Kwon, S.Y., Umbach, C.C., and Luo, D. (2006) *Nat. Mater.*, **5**, 797–801.

87. Park, N., Um, S.H., Funabashi, H., Xu, J., and Luo, D. (2009) *Nat. Mater.*, **8**, 432–437.

88. Rabe, K.S. and Niemeyer, C.M. (2009) *Nat. Mater.*, **8**, 370–372.